Molecular and Cellular Pathobiology

Cancer Research

NKX3.1 Activates Cellular Response to DNA Damage

Cai Bowen and Edward P. Gelmann

Abstract

The prostate-specific tumor suppressor homeodomain protein NKX3.1 is inactivated by a variety of mechanisms in the earliest phases of prostate carcinogenesis and in premalignant regions of the prostate gland. The mechanisms by which NKX3.1 exercises tumor suppression have not been well elucidated. Here, we show that NKX3.1 affects DNA damage response and cell survival after DNA damage. NKX3.1 expression in PC-3 prostate cancer cells enhances colony formation after DNA damage but has minimal effect on apoptosis. NKX3.1 also diminishes and regulates total cellular accumulation of γH2AX. Endogenous NKX3.1 in LNCaP cells localizes to sites of DNA damage where it affects the recruitment of phosphorylated ATM and the phosphorylation of H2AX. Knockdown of NKX3.1 in LNCaP cells attenuates the acute responses of both ATM and H2AX phosphorylation to DNA damage and their subnuclear localization to DNA damage sites. NKX3.1 expression enhances activation of ATM as assayed by autophosphorylation at serine 1981 and activation of ATR as assayed by phosphorylation of CHK1. An inherited mutation of NKX3.1 that predisposes to early prostate cancer and attenuates *in vitro* DNA binding was devoid of the ability to activate ATM and to colocalize with γH2AX at foci of DNA damage. These data show a novel mechanism by which a homeoprotein can affect DNA damage repair and act as a tumor suppressor. *Cancer Res; 70(8); 3089–97. ©2010 AACR.*

Introduction

NKX3.1 is a haploinsufficient prostate cancer suppressor protein that has reduced expression in the majority of human primary prostate cancers (1). NKX3.1 downregulation also predisposes to the formation of invasive prostate cancer and prostate carcinogenesis, because decreased expression is seen in premalignant lesions and prostatic intraepithelial neoplasia (1, 2). In mouse models, loss of *Nkx3.1* causes prostatic dysplasia and intraepithelial neoplasia but does not by itself cause invasive cancer. During prostate cancer progression, there is progressive loss of NKX3.1 expression, suggesting that there is an ongoing selective pressure against expression of this suppressor protein. Indeed, in up to 80% of metastatic prostate cancer foci, there is complete loss of NKX3.1 expression (3). NKX3.1 downregulation not only results from genetic loss, DNA methylation, or both, but also NKX3.1 turnover is accelerated by ubiquitination and proteasomal degradation triggered by cellular exposure to inflammatory cytokines, such as interleukin-1β and tumor necrosis factor-α (1, 4). In this way, regions of inflammatory atrophy may cause both downregulation of NKX3.1 and oxidative damage, which accompanies inflammation (2).

In trying to understand the mechanism by which NKX3.1 loss predisposes to prostate carcinogenesis, it was observed that NKX3.1 positively affects the expression of antioxidant enzymes and downregulates the expression of prooxidants, thereby acting to protect the cell and the genome from oxidative stress and DNA damage (5). NKX3.1 may also play a broader role in the cellular response to DNA damage. When we reported that NKX3.1 activated topoisomerase I, we observed that both proteins in concert changed their nuclear location in response to DNA-damaging agents. We have since pursued this observation by asking whether NKX3.1 affected cell survival after DNA damage and whether NKX3.1 was directly involved with the DNA damage response. In this report, we show that NKX3.1 expression has a protective effect against DNA-damaging agents. Moreover, NKX3.1 expression affects the activation of ATM and ATR, two members of the phosphoinositide 3-kinase (PI3K) family that activate the cell's response to DNA damage by initiating a signal transduction cascade.

Materials and Methods

Cell culture, transfection, and vectors. LNCaP, 293T, and PC-3 cells were cultured in IMEM (Invitrogen) supplemented with 10% fetal bovine serum (FBS; Invitrogen). Cells were transfected with either Lipofectamine 2000 (Invitrogen) or Fugene HD (Roche) according to manufacturer's instructions. Luciferase siRNA control and shNKX3.1 lentivirus vectors, which were custom-designed by Open Biosystems, were

Authors' Affiliation: Departments of Medicine and Pathology, Herbert Irving Comprehensive Cancer Center, Columbia University, New York, New York

Corresponding Author: Edward P. Gelmann, Departments of Medicine and Pathology, Herbert Irving Comprehensive Cancer Center, Columbia University, 177 Fort Washington Avenue, MHB 6N-435, New York, NY 10032. Phone: 212-305-8602; Fax: 212-305-3035; E-mail: gelmanne@columbia.edu.

doi: 10.1158/0008-5472.CAN-09-3138

stably transfected with Lipofectamine 2000 into LNCaP cell to generate LNCaP(siLuc), LNCaP(si471), and LNCaP (si3098) cell lines. The stable cell lines were selected with 5 μg/mL puromycin and maintained in media with 2 μg/mL puromycin.

Colony formation assay. For colony formation assay, PC-3 cells were transiently transfected with either empty pcDNA3 or pcDNA3-NKX3.1 and the cotransfected selection marker green fluorescent protein (GFP) with Lipofectamine 2000. Cells were sorted by fluorescence-activated cell sorting (FACS) based on expression of GFP, placed into six-well plates at 2,000 cells per well, and incubated in IMEM supplemented with 10% FBS for 24 h. Cells were subjected to treatment with UV, γ-irradiation, or mitomycin C for 1 h. Cells were incubated for 7 to 10 d to score for colony formation, fixed with 4% formaldehyde, and stained with crystal violet. All experiments were repeated. Apoptosis was assayed in PC-3(pcDNA3.1) and PC-3(NKX3.1) cells (6) after exposure to 10 mJ/cm^2 UV. Cells were fixed at indicated times by 4% formaldehyde, and apoptosis was detected by terminal deoxynucleotidyl transferase-mediated dUTP nick end labeling (TUNEL) assay (7).

Western blotting. Cell extracts were prepared by lysing cells with radioimmunoprecipitation assay buffer containing protease inhibitors (Complete mini, Roche) for detecting phosphorylation of proteins with phosphatase inhibitors (PhosStop, Roche). Proteins were resolved by SDS-PAGE and transferred to a nitrocellulose membrane. The primary antibodies used were polyclonal NKX3.1 (3), ATR (ABR), monoclonal anti-γH2AX (Upstate), anti-pATM-S1981 (Rockland), anti-pChk1-S345 (Cell Signaling), ATM (GeneTex), Chk1 (Santa Cruz), anti-β-actin (Sigma). The corresponding horseradish peroxidase–labeled secondary antibody was detected with SuperSignal West Pico Chemiluminescent substrate (Thermo Scientific) or SuperSignal West Dura Extended Duration Substrate (Thermo Scientific).

Immunofluorescence. Cells were fixed with 4% formaldehyde (Polysciences) or Streck Tissue Fixative in PBS for 15 min and permeabilized with either 0.5% Triton X-100 in PBS for 15 min at room temperature or ice-cold methanol for 10 min at −20°C. Cells were blocked with 3% bovine serum albumin (BSA) in PBS and incubated with primary antibody in 1% BSA in PBS followed by incubation with FITC-conjugated (Vector) or Alexafluor secondary antibody (Invitrogen). Cells were visualized with a Zeiss LSM 510 META scanning confocal microscope. Antibodies for immunofluorescence are polyclonal antibody against NKX3.1 (3), anti-ATR (C-19; Santa Cruz), monoclonal γH2AX (Upstate), anti-RAD51 (GeneTex), anti-poly(ADP- ribose) polymerase 1 (Biomol), anti-ATM (GeneTex), anti-pATM-S1981 (Rockland), and anti-53BP1 (Cell signaling).

Laser microirradiation. Cells were placed on polylysine-coated (Sigma) 35-mm glass bottomed microwell dishes (MatTek). Hoechst dye #33258 (Sigma) was added to the medium to a final concentration of 10 μg/mL. After 30 min of incubation at 37°C, the medium was aspirated from the cells, which were then washed and covered with phenol red–free IMEM supplemented with 10% FBS. A PALM MicroBeam IV Laser Capture Microdissection System (Zeiss) combined with laser scanning confocal microscopy was used for generation of local double-strand breaks by laser microirradiation and image acquisition. The energy output of the microdissection laser was 36%. After microirradiation, the recruitment of DNA repair proteins at defined DSB regions was identified by immunofluorescence as described above.

Results

We first determined whether NKX3.1 affected cell survival after DNA damage by assaying colony formation after cells were exposed to DNA-damaging agents. PC-3 prostate cancer cells were transiently transfected with either an empty expression vector or a plasmid expressing NKX3.1. Cells were cotransfected with a GFP expression vector used as a selection marker. After transfection, cells were subjected to DNA damage by exposure to UV, γ-irradiation, or mitomycin C. Cells were then sorted by FACS to select the transfected cells, and transfected and untransfected cells were then plated for colony formation. Transfection with NKX3.1 altered survival curves after DNA damage, as shown by increased colony formation after exposure to UV, γ-irradiation, and mitomycin C (Fig. 1A). The Western blot in Fig. 1A shows the expression of NKX3.1 in the transfected cells. The differences in colony formation were not due to an effect of NKX3.1 on apoptosis, as NKX3.1 expression did not affect induction of apoptosis in PC-3 cells (Fig. 1B).

One of the earliest indications of cellular response to DNA damage and an indicator of the degree of DNA damage, in particular double-stranded DNA breaks, is the phosphorylation of histone 2AX to form γ-histone 2AX (γH2AX; ref. 8). We examined the presence of γH2AX in PC-3 cells and PC-3(NKX3.1) cells during 6 hours after exposure to UV or mitomycin C. Expression of NKX3.1 attenuated the appearance of γH2AX over a 6-hour time span after exposure either to UV irradiation or mitomycin C (Fig. 2A). This result was consistent with the interpretation that more DNA damage accumulated in cells over 6 hours in the absence of NKX3.1 than in its presence. In a second experiment LNCaP cells that express endogenous NKX3.1 were subjected to NKX3.1 knockdown and in each of two independently derived LNCaP cell lines, LNCaP(si471) and LNCaP(si3098). Knockdown of NKX3.1 expression is shown in Fig. 2B (bottom). Knockdown of NKX3.1 resulted in increased accumulation of γH2AX over 6 hours (Fig. 2B). Thus, NKX3.1 expression correlated with decreased overall accumulation of γH2AX.

The DNA damage response and phosphorylation of γH2AX by ATM and ATR occurs within minutes of DNA strand breakage. To examine the effect of NKX3.1 on the shorter-term response of cells to DNA damage, LNCaP cells and NKX3.1 knockdown cells were examined at 10 and 30 min after exposure of BrdUrd-treated cells to UV irradiation. BrdUrd sensitizes DNA to UV and predisposes to UV-induced double-stranded DNA breakage. LNCaP(siLuc) cells showed expression of NKX3.1 by immunohistochemical staining, which was substantially decreased in LNCaP (si471) cells (Fig. 3A, compare panels b). Within 10 minutes after exposure to UV LNCaP(siLuc), cells showed formation

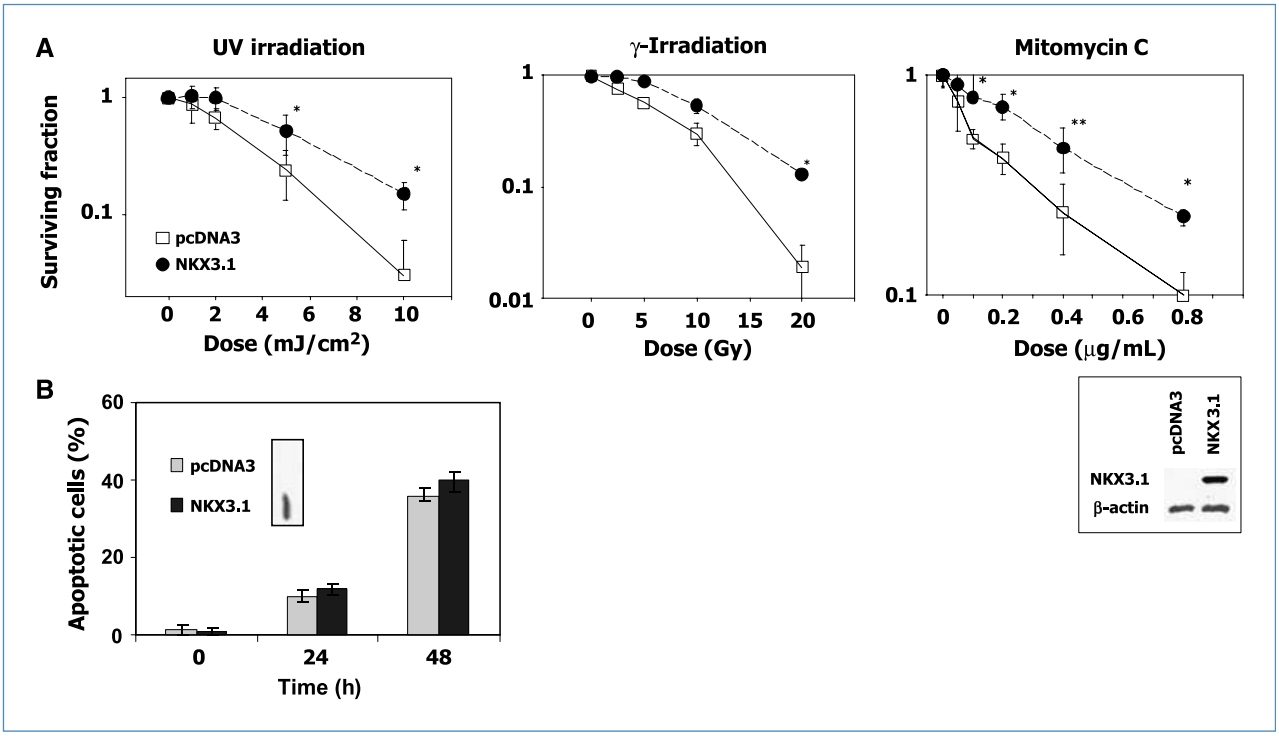

Figure 1. NKX3.1 affects colony formation after exposure of PC-3 cells to DNA-damaging agents. A, PC-3 cells were cotransfected with either pcDNA3 or pcDNA3(NKX3.1) and a GFP expression plasmid and were sorted by FACS. Both GFP-positive and GFP-negative cells were placed into six-well plates at 2,000 cells per well. Cells were incubated in IMEM supplemented with 10% FBS for 24 h. Cells were subjected to UV, γ-irradiation, or mitomycin C for 1 h at the doses and exposures shown. Colony formation was counted 7 to 10 d later. The surviving fraction at each data point was normalized by comparison to colony formation without any treatment. Bottom right, the expression of NKX3.1 in sorted cells to show the efficacy of FACS selection for the cotransfected marker. B, PC-3 cells stably transfected with either pcDNA3 or NKX3.1 expression vector were exposed to 10 mJ/cm^2 UV and assayed at 24 and 48 h for apoptosis by TUNEL assay.

of γH2AX foci as shown at both lower power and higher power (Fig. 3A, compare d and g for both derivative cells). Figure 3A (g–i) shows in a higher power view of a single nucleus that staining of γH2AX and NKX3.1 aggregated in granular regions. The insets for LNCaP(siLuc) show magnified views of the regions marked with the arrow heads (Fig. 3A, left, g–l). In contrast, there was minimal formation of γH2AX foci in LNCaP(si471) cells at 10 minutes after UV exposure (Fig. 3A, right, d and g). γH2AX focus formation in LNCaP (si471) cells was seen to have increased at 30 minutes after UV exposure (Fig. 3A, right, compare j and g). This was in contrast to γH2AX focus formation in LNCaP(siLuc) cells that had plateaued by 30 minutes (Fig. 3A, 30-minute panels j–l and B, graph on the left). Expression of NKX3.1 in LNCaP (siLuc) cells was also associated with a more rapid response to DNA damage as measured by the fraction of γH2AX-positive cells (Fig. 3B, right, graph). In contrast, the fraction of γH2AX-positive LNCaP(si471) cells increased more slowly and was still rising at 30 minutes after exposure to UV irradiation (Fig. 3B, right, graph).

H2AX is a target for phosphorylation by the PI3K family members ATM and ATR that are activated in response to a variety of stimuli, including DNA breaks (9, 10). Thus, the effect of NKX3.1 on the phosphorylation of H2AX suggested that NKX3.1 affected the activity of ATM, ATR, or both. The effect of NKX3.1 on the formation of ATM and ATR nuclear complexes after DNA damage was studied in LNCaP cells expressing either siLuc or si471. Ten minutes after exposure to mitomycin C, ATM, ATR, and γH2AX nuclear foci were seen in the presence of NKX3.1 as shown by confocal immunofluorescent microscopy of the single nucleus shown in Fig. 4A. As in Fig. 3A, effective knockdown of NKX3.1 expression was seen in the LNCaP(si471) cells (Fig. 4A, b, e, and h). Each panel in Fig. 4A shows a single nucleus in which NKX3.1, γH2AX, ATM, and ATR aggregate after the cells were exposed to irradiation. At higher magnification (figure insets), colocalization of NKX3.1 with γH2AX, ATM, and ATR is seen in nuclear granules marked with arrows in the lower power images. However, in the presence of NKX3.1 knockdown, very few γH2AX, ATM foci, or ATR foci were seen at the 10-minute time point (Fig. 4A, right, a–i). Quantitation of the nuclear focus formation in cells at 10 minutes is seen in Fig. 4B. NKX3.1 knockdown resulted in a decreased number of detectable foci per nucleus (Fig. 4B, left) and a decrease in the fraction of cells with visible signals (Fig. 4B, right).

Recognition of and response to DNA damage occurs within seconds to a few minutes of DNA damage. To determine whether NKX3.1 affected the immediate response to DNA

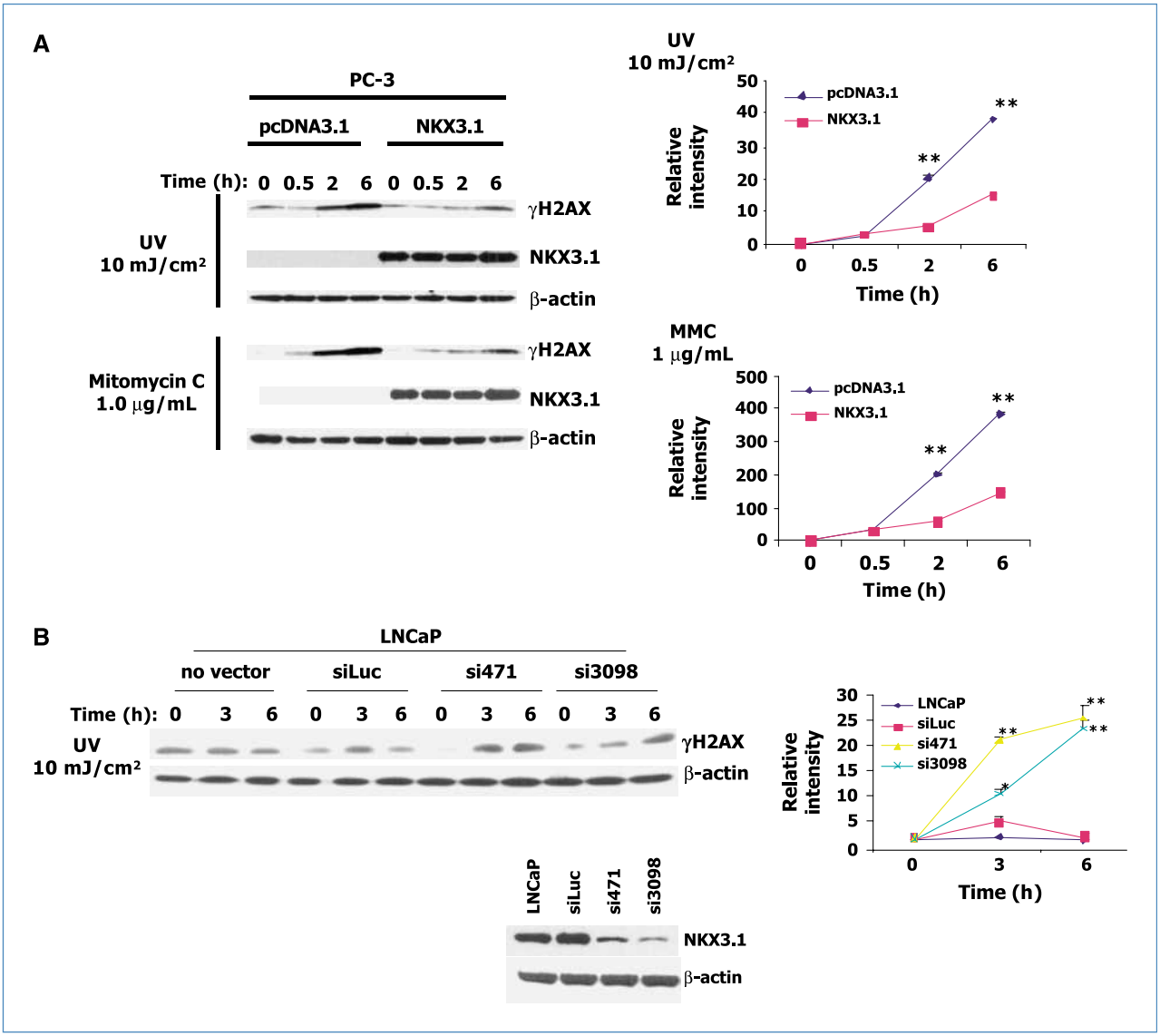

Figure 2. NKX3.1 expression affects total γH2AX accumulation after DNA damage. A, PC-3 cells transiently transfected with pcDNA3 or pcDNA3-NKX3.1 plasmids were treated with 10 mJ/cm^2 of UV or 1 μg/mL of mitomycin C for 1 h. Cells were collected at the indicated times after treatment. Cell lysates were resolved by SDS-PAGE and probed with antibodies to γH2AX, NKX3.1, and β-actin. Signal intensity was measured and quantified by Image J software. Relative phosphorylation of H2AX was calculated by normalizing the intensity of γH2AX of each lane to that of the untreated sample. B, LNCaP, LNCaP(siLuc), LNCaP(si471), and LNCaP(si3098) were subjected to 10 mJ/cm^2 of UV treatment. Cells were harvested at the indicated times and processed for Western blotting. The effect of NKX3.1 siRNA is shown in the Western blot (bottom).

damage, we used laser microirradiation of LNCaP(si471) cells transfected with different MYC-tagged NKX3.1 constructs. We expressed MYC-tagged NKX3.1 and two constructs with inactivating mutations in the homeodomain. One mutant expression construct, MYC-tagged NKX3.1(T164A), coded a protein found in a family with hereditary early incidence of prostate cancer (11). The missense mutation alters the α-helical cap amino acid of the third helix of the homeodomain and diminishes DNA binding to 5% of the wild-type protein. A second NKX3.1 construct with a missense mutation in the homeodomain (N174Q) was also studied. Asparagine 51 of the *Drosophila* NK-2 homeodomain is juxtaposed to the major groove of DNA when the protein binds to its cognate hexanucleotide (12). A missense mutation changing asparagine 174 at the 51st amino acid of the homeodomain to glutamine (N174Q) reduces DNA binding by a factor of >10^{-3}.[1]

MYC-tagged NKX3.1 was expressed in LNCaP(si471) cells by transient transfection, and cells, pretreated with Hoechst 33258 dye, were subject to laser microirradiation to induce double-stranded DNA breaks in response to UV. Expression of MYC-NKX3.1 was seen with MYC antibody, and MYC-NKX3.1

[1] Our unpublished observation.

localized to the site of UV irradiation. This was not seen in untransfected cells (Fig. 5A, e and f). MYC-NKX3.1 enhanced the formation of γH2AX at the site of UV within 2 to 3 minutes of double-stranded DNA damage (Fig. 5A, compare a and b). Moreover, MYC-NKX3.1 and γH2AX were seen to colocalize at the site of UV (Fig. 5A, compare i and j). Both MYC-NKX3.1(T164A) and MYC-NKX3.1(N174Q) were expressed in LNCaP(si471) cells but did not accumulate the sites of laser microirradiation (Fig. 5A, g and h, respectively). γH2AX was seen to accumulate in the laser microirradiation sites of both transfected and untransfected cells, but there was no difference in intensity of γH2AX staining between cells expressing the NKX3.1 mutant constructs and those that did not (Fig. 5A, c and d). Also, the mutant NKX3.1 proteins did not localize to the regions of DNA damage (Fig. 5A, g and h) and did not colocalize with γH2AX (Fig. 5A, k and l).

Before phosphorylation of γH2AX, the PI3K-like protein ATM is rapidly phosphorylated on serine 1981 in response to DNA damage (13). To determine whether NKX3.1 affected phosphorylation of ATM, we examined the appearance of pATM-S1981 in the presence of different NKX3.1 constructs within 1 to 3 minutes of DNA damage induced by laser microirradiation. In the top row of images in Fig. 5B, pATM-S1981 is seen to accumulate at the sites of damage in all three cell lines. The fluorescent signal was strongest in cells expressing wild-type MYC-NKX3.1 (Fig. 5B, a, b, and c). As seen in Fig. 5A,

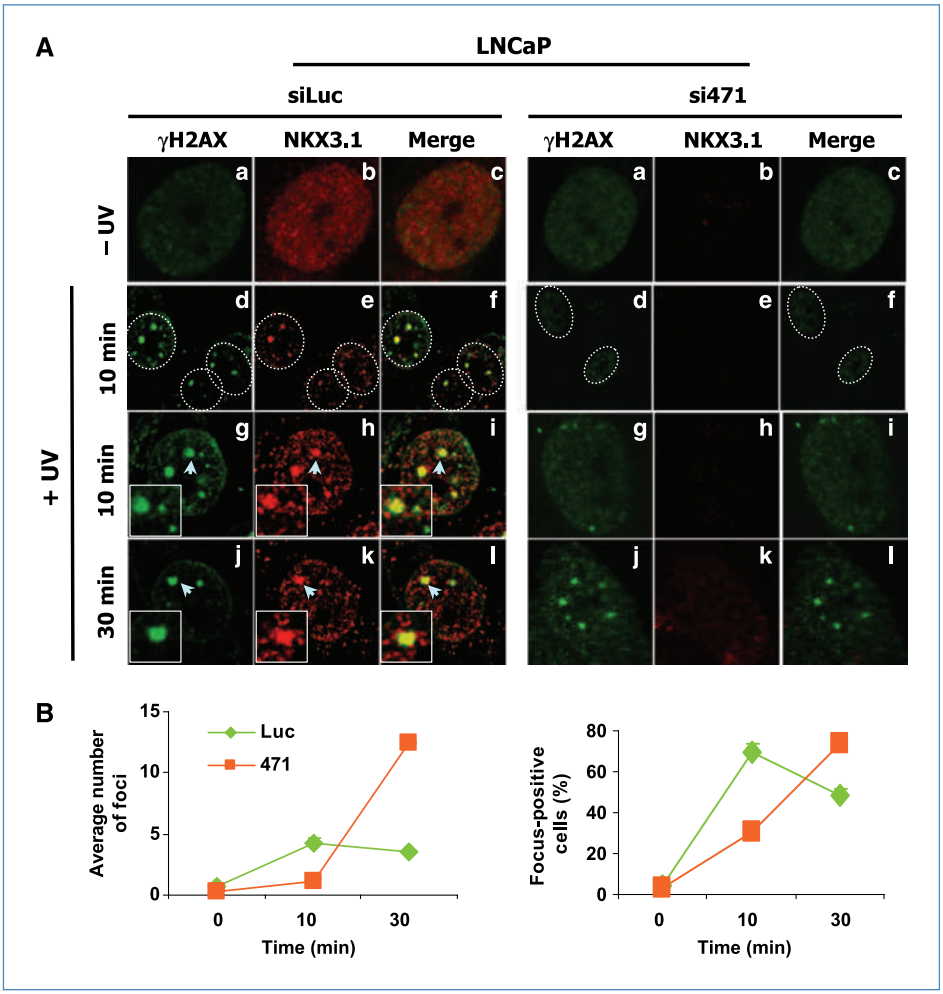

Figure 3. Effect of NKX3.1 knockdown on γH2AX accumulation after induction of double-stranded DNA breaks. LNCaP(siLuc) and LNCaP(si471) cells were treated with BrdUrd and subjected to 10 mJ/cm^2 UV irradiation. Cells were fixed at indicated times with 4% formaldehyde and permeabilized with 0.5% Triton X-100 in PBS for 15 min. γH2AX focus formation and colocalization of γH2AX with NKX3.1 were revealed using monoclonal γH2AX antibody and polyclonal NKX3.1 antibody for 1 h incubation at room temperature and then followed by overnight incubation at 4°C. FITC conjugated secondary antibody or biotinylated secondary antibody and subsequent avidin–Texas red incubation were used for detecting γH2AX and NKX3.1, respectively. A, a single unirradiated cell is shown in the top row of images. The 10-min time point is represented by lower power images with several cells in the second row. Nuclei are shown circled by dotted lines. Higher power images of a single nucleus are shown in the third row. The insets at the 10-min time point display an amplified image of the colocalization of γH2AX and NKX3.1 in nuclear foci. The 30-min time point is shown in the fourth row where foci of γH2AX are more readily seen in LNCaP(si471) cells. B, the average number of foci in cells (left) and percentage of focus-positive cells (right) were obtained by counting 100 cells for each cell sample. The experiment was one of two with nearly identical results.

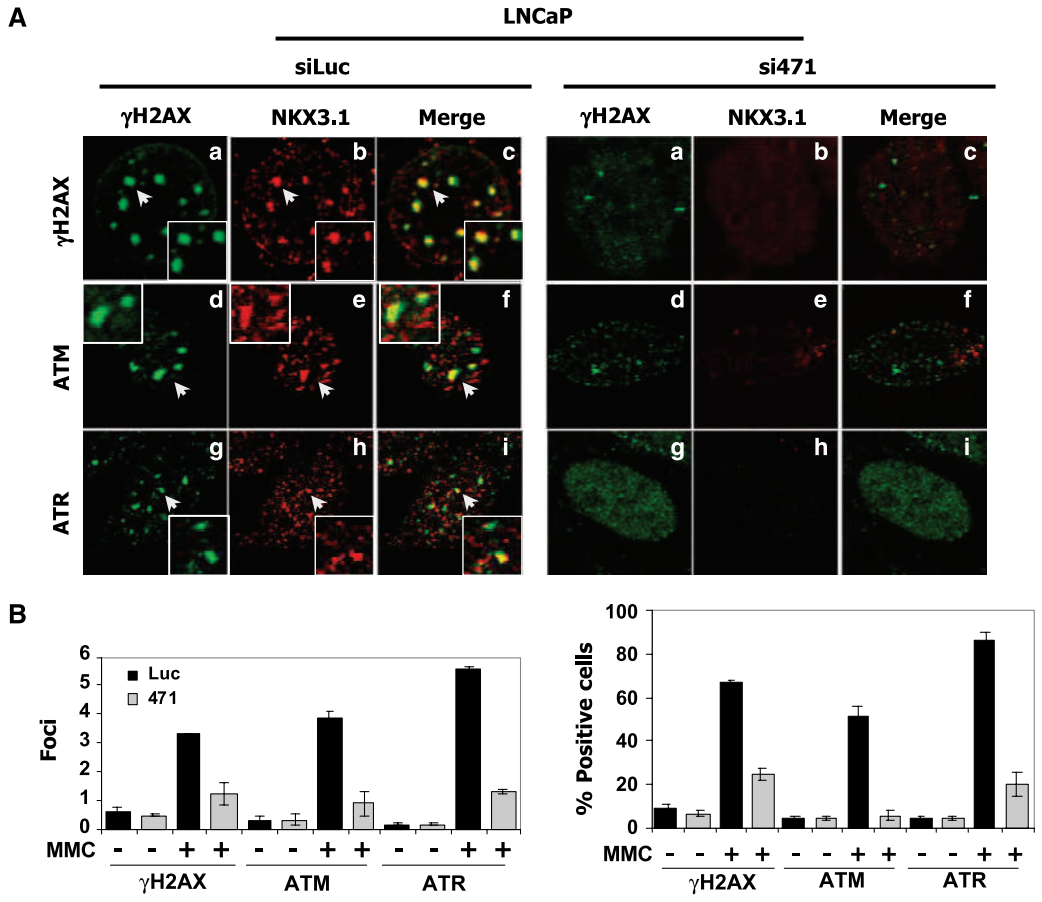

Figure 4. NKX3.1 mediates ATM and ATR localization in the early DNA damage response. LNCaP(siLuc) and LNCaP(si471) cells placed on polylysine-coated 35-mm dishes were treated with 1 μg/mL of mitomycin C for 10 min. Cells were fixed by STF fixative (for ATR with methanol) and then permeabilized with 0.5% Triton X-100 for 15 min. Foci were detected with polyvalent antiserum against NKX3.1, anti-ATR, monoclonal anti-γH2AX, and anti-ATM antibodies. Secondary antibodies are Alexa Fluor 568 and FITC conjugated. A, images of a single nucleus are shown with staining of intranuclear granules for γH2AX, ATM, ATR, and NKX3.1. The insets in the LNCaP(siLuc) images display colocalization of γH2AX, ATM, or ATR with NKX3.1 in nuclear foci designated by the arrows in the main panels. In LNCaP(si471) cells, NKX3.1 staining is markedly diminished and intranuclear focus formation is attenuated at the 10-min time point. B, focus formation was visualized on laser scanning confocal microscope and quantified with Image J software. Average foci number in cells and percentage of foci-positive cells were acquired by counting 100 cells. The *X* axis labels apply to both the top and bottom histograms. A repeated experiment showed a nearly identical result.

wild-type MYC-NKX3.1, but not mutant protein, localized to the site of UV irradiation (Fig. 5B, d, e, and f). In the merged images at the bottom, colocalization of MYC-NKX3.1 and pATM-S1981 is seen, but not the mutant proteins (Fig. 5B, g, h, and i). This result is consistent with the notion that NKX3.1 expression facilitates activation of ATM and downstream phosphorylation of H2AX. Thus NKX3.1 affects the earliest stages of the cellular DNA damage response.

To show further the effect of NKX3.1 expression on DNA damage response by assaying cellular levels of activated ATM and ATR, we did Western blotting of cell extracts after exposure to mitomycin C (Fig. 6A). NKX3.1 knockdown is seen in the Western blot with NKX3.1 antibody. Knockdown of NKX3.1 markedly attenuated phosphorylation of ATM. In addition, LNCaP(si471) cells had decreased activation of ATR as shown by diminished phosphorylation of the ATR target CHK1 at serine 345 (14). Importantly, NKX3.1 did not affect protein levels of the DNA response kinases but rather seemed to affect kinase activation and downstream signaling. Further demonstration that the effect of NKX3.1 on ATM and ATR activation was not due to off-target effects of the siRNAs was seen in PC-3 cells transfected with NKX3.1 and subjected to UV irradiation after treatment with Hoechst dye. NKX3.1 expression accelerated activation of ATM in PC-3 cells (Fig. 6B).

Discussion

A substantial weight of evidence now implicates NKX3.1 as a key tumor suppressor and the lead candidate for the gatekeeper of prostate cancer (15). This haploinsufficient protein has been shown in mouse models to be a critical determinant of prostate epithelial differentiation and growth

control (16–19). In premalignant lesions NKX3.1 protein levels are subjected to reductions due to the actions of inflammatory cytokines (2, 4). In human prostate cancer, NKX3.1 is subject to reductions in levels of cellular protein by gene methylation and loss of heterozygosity (1). Numerous studies have shown that loss of the 8p21 locus, including *NKX3.1* is a very common event in human prostate cancer accounting for *NKX3.1* loss in a majority of cases (20, 21). In human cancer specimens, levels of NKX3.1 protein vary widely around a median level of 0.67 of expression in the adjacent normal prostate epithelium. Interestingly, $Nkx3.1^{+/-}$ mice have a level of Nkx3.1 protein in prostate epithelium that is also 0.67 of wild-type levels, suggesting that the residual contralateral allele compensates somewhat for loss of one gene copy (1). Nevertheless, it is apparent that a variety of factors influence NKX3.1 protein levels in human prostate epithelium.

Our data show that expression of NKX3.1 affects early events in the response to DNA damage and results in increased cell survival and clonogenicity. Conversely, decreased levels of NKX3.1 attenuate the acute response to DNA damage and extend the time during which the cell activates phosphorylation of H2AX, presumably due to an extended time for recognition and remediation of DNA strand breaks. This is an important example of a homeodomain protein directly influencing detection of DNA damage and the DNA repair process. The effect of NKX3.1 on DNA repair may be by direct interaction with DNA repair proteins or by an indirect effect. Experiments to address this point are well under way in our laboratory. Knockdown of NKX3.1 affected the DNA damage response. This effect was not due to off-target effects of siRNA for at least two reasons. In Fig. 5, MYC-NKX3.1 was expressed in LNCaP(si471) knockdown cells and reversed the effect of NKX3.1 knockdown on the DNA damage response. We also studied ATM activation in derivative PC-3 cells to show that NKX3.1 expression affected the timing of ATM phosphorylation after DNA damage.

NKX3.1 has a manifold role in both protecting and repairing DNA, suggesting that DNA protection and integrity may be essential elements of its role in the cell. We previously showed that NKX3.1 binds to topoisomerase I and enhances its DNA-binding and supercoil resolving activity in a stoichiometric fashion (22). By interacting with topoisomerase I, NKX3.1 may also affect DNA integrity because topoisomerase I has been implicated in DNA repair. Topoisomerase I colocalizes with P53 at sites of DNA damage in response to UV irradiation (23). Moreover, knockdown of topoisomerase I predisposes cells to chromosomal instability, suggesting that topoisomerase I has an ongoing function in maintenance of DNA integrity (24). Our findings represent the second example of a homeodomain protein interacting with DNA repair enzymes. The HOXB7 homeodomain protein that functions in body axis patterning is able, when overexpressed, to transform mammary epithelial cells and enhance nonhomologous end-joining after DNA damage. HOXB7 was shown to interact with components of the DNA-dependent protein kinase holoenzyme via helix 3 of its homeodomain (25).

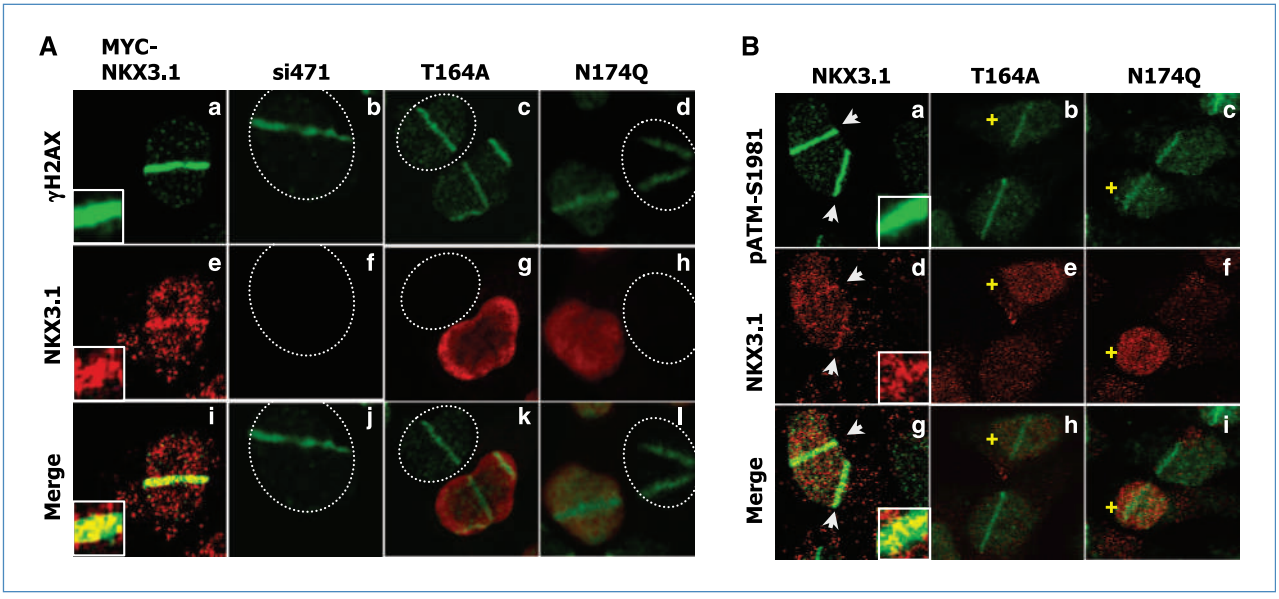

Figure 5. NKX3.1 affects the immediate response to DNA damage. A, LNCaP(si471) cells transiently transfected with MYC-tagged NKX3.1 expression plasmids as shown with Lipofectamine 2000 were pretreated with 10 μg/mL Hoechst dye for 30 min and then supplemented with phenol red–free IMEM with 10% FBS. Cells were subjected to laser microirradiation and fixed 2 to 5 min posttreatment. Immunofluorescence was performed as described in Materials and Methods. γH2AX was detected with monoclonal γH2AX antibody. NKX3.1 was detected with polyvalent antiserum. A, images show one or two nuclei. LNCaP(si471) cells not transfected with MYC-NKX3.1 plasmids and therefore not stained with MYC antibody are circled. The NKX3.1-positive nucleus in h is not fully in focus to get correct focus on the adjacent NKX3.1-negative cell. The insets in a, e, and i display higher power images of the sites of DNA damage showing colocalization of γH2AX and wild-type NKX3.1. B, same as in A only with detection of pATM-S1981. The insets in a, d, and g display magnified images of the sites of DNA damage showing colocalization of pATM-S1981 and wild-type NKX3.1. The + signs in panels b, e, and h designated NKX3.1 expressing cells.

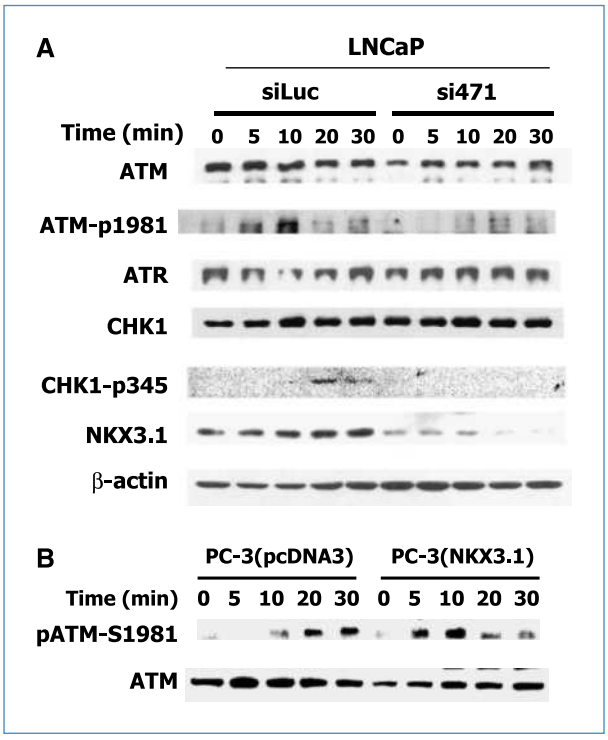

Figure 6. NKX3.1 activates ATM and ATR signaling. A, LNCaP(siLuc) and LNCaP(si471) cells were treated with 1 μg/mL mitomycin C for the indicated times. Cell extracts were isolated and resolved by SDS-PAGE. The activation of ATM and ATR pathways was detected by Western blotting. B, PC-3 derivative cells were exposed to 10 mJ/cm^2 of UV irradiation after preincubation with 10 μg/mL Hoechst 33258 dye for 30 min. Cell extract was isolated at indicated times, and Western blotting was performed with monoclonal anti-pATM-S1981 (Rockland) or anti-ATM (GeneTex) antibodies.

The role of NKX3.1 in maintaining DNA stability is further suggested by studies in gene-targeted mice, wherein Nkx3.1 expression affects the transcriptional profile of a range of prooxidant and antioxidant enzymes and dysplastic prostate epithelium of *Nkx3.1* deletion mice has increased levels of 8-oxoguanine (5). The effect of Nkx3.1 on transcription of genes that affect oxidative stress is likely to occur via indirect mechanisms. Although, as is expected of a homeodomain-containing protein, NKX3.1 binds to DNA (26). However, NKX3.1 cannot initiate formation of a transcription complex and by itself does not activate transcription but rather suppresses transcription when targeted to a promoter region by placement of cognate DNA-binding sequences (26). Transcriptional activation by NKX3.1 is seen when NKX3.1 serves as a coactivator for transcription factors like serum response factor. NKX3.1 binds both to DNA sequences adjacent to the serum response element (27) and to SRF directly (28). Protein-protein interaction between NKX3.1 and SRF is mediated by the homeodomain and influenced by NH_2 and COOH terminal flanking regions of the protein (28).

Many activities of NKX3.1 are mediated by interactions of other proteins with the homeodomain. The homeodomain is the locus for interaction with the major groove of DNA and responsible for DNA binding (11, 12, 28). However, the NKX3.1 homeodomain is also the site of interaction with proteins, such as topoisomerase I. In fact, topoisomerase I was able to titrate NKX3.1 off its cognate DNA-binding sequence (22). Our results suggest that the homeodomain is also important for the effect of NKX3.1 on early steps in DNA break recognition. A construct that had lost 95% or more of wild-type DNA-binding affinity had essentially no detectable effect on DNA break recognition.

Our finding that NKX3.1 plays a role in maintaining DNA integrity of prostate epithelial cells is consistent with the notion that decreased levels of NKX3.1 in premalignant prostate tissue may predispose to accumulation of mutations and transformation to prostate cancer. If regions of inflammatory atrophy are present throughout the prostate gland then it follows there may be multiple independent oncogenic events leading to independent foci of transformed epithelial cells. This prediction is supported by analyses of prostatectomy specimens that showed multiple foci of cancer with distinct genetic signatures in a single gland (29). Thus, we envision that stochastic inflammatory foci in the prostate result in reductions of NKX3.1 half-life in adjacent prostate epithelial cells, diminishing the response to DNA damage. Inflammation also increases the local production of reactive oxygen species, thus leading to the formation of 8-oxoguanine and subsequent mutations. Decreased levels of NKX3.1 also decrease the production of antioxidant enzymes and increase the synthesis of prooxidant enzymes, further exacerbating the chance of mutagenesis and facilitating steps to carcinogenesis. Our report that NKX3.1 affects DNA integrity in prostate epithelial cells thus adds further evidence to the critical role this protein plays in the pathogenesis of prostate cancer.

Disclosure of Potential Conflicts of Interest

No potential conflicts of interest were disclosed.

Acknowledgments

The costs of publication of this article were defrayed in part by the payment of page charges. This article must therefore be hereby marked *advertisement* in accordance with 18 U.S.C. Section 1734 solely to indicate this fact.

Received 08/24/2009; revised 12/22/2009; accepted 01/21/2010.

References

1. Asatiani E, Huang WX, Wang A, et al. Deletion, methylation, and expression of the NKX3.1 suppressor gene in primary human prostate cancer. Cancer Res 2005;65:1164–73.
2. Bethel CR, Faith D, Li X, et al. Decreased NKX3.1 protein expression in focal prostatic atrophy, prostatic intraepithelial neoplasia, and adenocarcinoma: association with Gleason score and chromosome 8p deletion. Cancer Res 2006;66:10683–90.
3. Bowen C, Bubendorf L, Voeller HJ, et al. Loss of NKX3.1 expression

in human prostate cancers correlates with tumor progression. Cancer Res 2000;60:6111–5.
4. Markowski MC, Bowen C, Gelmann EP. Inflammatory cytokines induce phosphorylation and ubiquitination of prostate suppressor protein NKX3.1. Cancer Res 2008;68:6896–901.
5. Ouyang X, DeWeese TL, Nelson WG, Abate-Shen C. Loss-of-function of Nkx3.1 promotes increased oxidative damage in prostate carcinogenesis. Cancer Res 2005;65:6773–9.
6. Muhlbradt E, Asatiani E, Ortner E, Wang A, Gelmann EP. NKX3.1 activates expression of insulin-like growth factor binding protein-3 to mediate insulin-like growth factor-I signaling and cell proliferation. Cancer Res 2009;69:2615–22.
7. Kimura K, Bowen C, Spiegel S, Gelmann EP. Tumor necrosis factor-α sensitizes prostate cancer cells to γ-irradiation-induced apoptosis. Cancer Res 1999;59:1606–14.
8. Rogakou EP, Pilch DR, Orr AH, Ivanova VS, Bonner WM. DNA double-stranded breaks induce histone H2AX phosphorylation on serine 139. J Biol Chem 1998;273:5858–68.
9. Ward IM, Chen J. Histone H2AX is phosphorylated in an ATR-dependent manner in response to replicational stress. J Biol Chem 2001;276:47759–62.
10. Burma S, Chen BP, Murphy M, Kurimasa A, Chen DJ. ATM phosphorylates histone H2AX in response to DNA double-strand breaks. J Biol Chem 2001;276:42462–7.
11. Zheng SL, Ju JH, Chang BL, et al. Germ-line mutation of NKX3.1 cosegregates with hereditary prostrate cancer and alters the homeodomain structure and function. Cancer Res 2006;66:69–77.
12. Gruschus JM, Tsao DH, Wang LH, Nirenberg M, Ferretti JA. Interactions of the vnd/NK-2 homeodomain with DNA by nuclear magnetic resonance spectroscopy: basis of binding specificity. Biochemistry 1997;36:5372–80.
13. Bakkenist CJ, Kastan MB. DNA damage activates ATM through intermolecular autophosphorylation and dimer dissociation. Nature 2003;421:499–506.
14. Liu Q, Guntuku S, Cui XS, et al. Chk1 is an essential kinase that is regulated by Atr and required for the G(2)/M DNA damage checkpoint. Genes Dev 2000;14:1448–59.
15. Abate-Shen C, Shen MM, Gelmann E. Integrating differentiation and cancer: the Nkx3.1 homeobox gene in prostate organogenesis and carcinogenesis. Differentiation 2008;76:717–27.
16. Bhatia-Gaur R, Donjacour AA, Sciavolino PJ, et al. Roles for Nkx3.1 in prostate development and cancer. Genes Dev 1999;13:966–77.
17. Kim MJ, Cardiff RD, Desai N, et al. Cooperativity of Nkx3.1 and Pten loss of function in a mouse model of prostate carcinogenesis. Proc Natl Acad Sci U S A 2002;99:2884–9.
18. Kim MJ, Bhatia-Gaur R, Banach-Petrosky WA, et al. Nkx3.1 mutant mice recapitulate early stages of prostate carcinogenesis. Cancer Res 2002;62:2999–3004.
19. Abate-Shen C, Banach-Petrosky WA, Sun X, et al. Nkx3.1; Pten mutant mice develop invasive prostate adenocarcinoma and lymph node metastases. Cancer Res 2003;63:3886–90.
20. Swalwell JI, Vocke CD, Yang Y, et al. Determination of a minimal deletion interval on chromosome band 8p21 in sporadic prostate cancer. Genes Chromosomes Cancer 2002;33:201–5.
21. Lapointe J, Li C, Giacomini CP, et al. Genomic profiling reveals alternative genetic pathways of prostate tumorigenesis. Cancer Res 2007;67:8504–10.
22. Bowen C, Stuart A, Ju JH, et al. NKX3.1 homeodomain protein binds to topoisomerase I and enhances its activity. Cancer Res 2007;67:455–64.
23. Mao Y, Muller MT. Down modulation of topoisomerase I affects DNA repair efficiency. DNA Repair (Amst) 2003;2:1115–26.
24. Miao ZH, Player A, Shankavaram U, et al. Nonclassic functions of human topoisomerase I: genome-wide and pharmacologic analyses. Cancer Res 2007;67:8752–61.
25. Rubin E, Wu X, Zhu T, et al. A role for the HOXB7 homeodomain protein in DNA repair. Cancer Res 2007;67:1527–35.
26. Steadman DJ, Giuffrida D, Gelmann EP. DNA-binding sequence of the human prostate-specific homeodomain protein NKX3.1. Nucleic Acids Res 2000;28:2389–95.
27. Carson JA, Fillmore RA, Schwartz RJ, Zimmer WE. The smooth muscle γ-actin gene promoter is a molecular target for the mouse bagpipe homologue, mNkx3-1, and serum response factor. J Biol Chem 2000;275:39061–72.
28. Ju JH, Maeng JS, Zemedkun M, et al. Physical and functional interactions between the prostate suppressor homeoprotein NKX3.1 and serum response factor. J Mol Biol 2006;360:989–99.
29. Bostwick DG, Shan A, Qian J, et al. Independent origin of multiple foci of prostatic intraepithelial neoplasia: comparison with matched foci of prostate carcinoma. Cancer 1998;83:1995–2002.